Available online at www.eccomasproceedia.org
Eccomas Proceedia COMPDYN (2019) 409-421

ECCOMAS
Proceedia

COMPDYN 2019
7th ECCOMAS Thematic Conference on
Computational Methods in Structural Dynamics and Earthquake Engineering
M. Papadrakakis, M. Fragiadakis (eds.)
Crete, Greece, 24–26 June 2019

SHEAR PLASTIC OSCILLATIONS OF A WIND TURBINE TOWER

Michela Monaco[1], Anna Tafuro[1], Bruno Calderoni[2], Mariateresa Guadagnuolo[1]

[1]Department of Architecture and Industrial Design, University of Campania L. Vanvitelli
Via San Lorenzo 1, 81031Aversa (CE), Italy
e-mail: {michela.monaco; anna.tafuro; mariateresa.guadagnuolo}@unicampania.it

[2] Department of Structure for Engineering and Architecture, University of Naples Federico II
Via Claudio 21, 80125 Napoli, Italy
calderon@unina.it

Abstract

The vulnerability of wind turbine towers is an actual theme, considered the recent diffusion of aeolian parks. In many cases collapses of wind towers after severe actions have been observed. The analysis of structures subjected to variable actions can be performed by means of several methods with different levels of accuracy. Nonlinear dynamics is generally considered the most reliable one. This paper presents a numerical procedure for the analysis of rigid-plastic response of a wind turbine tower, considered a cantilever beam subjected to harmonic forcing motion of the base support. The failure is assumed depending on the formation shear hinges and the results are expressed in general terms for application to real cases. The proposed model is an evolution of the cantilever model with a single degree of freedom, since the plastic hinges can form in every section of the beam. For the solution of the problem, a numerical procedure has been developed that provides simple relationships between the strength of the structure and parameters useful for design purposes. The approach presents the advantages of rigid-plastic procedure and an efficient representation of the post-elastic behaviour of the structure, low computational competence and limited number of mechanical parameters are involved.

Keywords: Nonlinear dynamics, plastic shear failure, modal approximation, time history.

ISSN:2623-3347
Peer-review under responsibility of the organizing committee of COMPDYN 2019.
doi: 10.7712/120119.6928.19511

1 INTRODUCTION

The need of clear energy has enhanced the diffusion of the aeolian parks, i.e. sets of modern wind turbine for the production of electric power. Several of these parks have been realized in seismic areas. Many of them have been built in Irpinia, a region of Southern Italy devastated by a strong earthquake in 1980. Recent collapses of wind towers after severe actions (Figure 1) has lead to the search of reliable tool to examine the effects of earthquake actions on these structures [1].

Nonlinear dynamics can be a one of these, although it needs a great level of expertise, as well as cost and time necessary for calculation [2].

In general when the elastic response can be disregarded and micromechanical behaviour involves complex experimental tests, constitutive and structural models with sufficient accuracy and low numerical complexities are useful [3, 4]. Among them, rigid-plastic approximations, largely diffused in earthquake engineering, give rise to simplified procedures [5], although its implementation within conventional stiffness-based computer methods, the instantaneous jump of stiffness between zero and infinite. The model examined in this paper, together with those developed for rigid-plastic bending frames, overcomes this last limit [6, 7]. In literature, in fact, constitutive models for rigid-plastic bending frames are diffused, differently from the shear constitutive ones. A large amount of literature exists in fact for the dynamic plastic bending response of structural elements, both steel and reinforced concrete structures. Bending hinges represent in fact general response characteristics of several structural elements under transverse load [8, 9]. A minor number of papers concerning dynamic analyses of plastic shear failure can be found. The key aspect to be studied in both the bending and shear problems is the localization and extension of plastic hinges.

Figure 1: Collapsed wind tower [18]

In a nonlinear dynamic analysis the rigid-plastic cantilever beam can be a simple structural scheme to model the behaviour of more complex structures [10]. The single-degree-of-freedom model provides a preliminary assessment of the structure and a good estimation of the response mode [11], which is normally responsible for overall structural failure, as in the case of wind turbine towers in near fault ground motions. These motions are often characterized by pulse sequences with simple shapes that can be recognized in the accelerograms by means of spectral analysis [12]. The acceleration pulse responsible for most of the inelastic deformations of structures can be distinguished among them [13].

In general if accurate harmonic pulses are used to represent the ground motion the development of elastic and inelastic response spectra are facilitated [14]. These considerations are

the basis of the numerical analysis performed, since the harmonic pulse can be a suitable representation of near-fault ground motions [15].

The rigid-plastic dynamic response of slender structures subjected to base pulse is examined in this paper [16]. The case study is a wind turbine tower considered like a cantilever beam subjected to harmonic forcing motion of the base support. The failure is assumed depending on the formation shear hinges and the results are expressed in general terms for application to real cases. The proposed model is an evolution of the SDOF cantilever beam, since the plastic hinges can form in every section of the beam. For the solution of the problem, a numerical procedure has been developed that provides simple relationships between the strength of the structure and parameters useful for design purposes.

2 GENERAL THEORETICAL MODEL

Rigid-plastic models allow simpler solutions than elastic-plastic theory [17], so that approximated methods adopting the rigid-plastic models are useful in case of estimate of major deformations due to very large dynamic loads. This estimation can be successively refined to include the initially neglected aspects. In what follows geometry changes are small and the yield stress is assumed to be independent on the strain rate. Reference is made to the elastic perfectly plastic body in Figure 2.

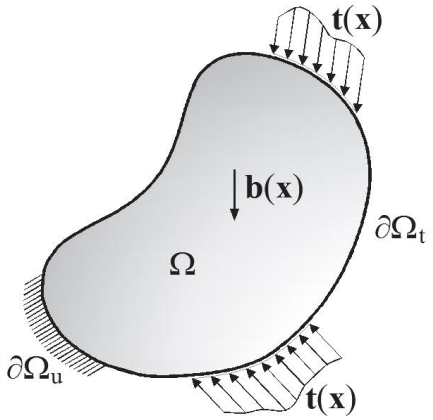

Figure 2: The elastic perfectly plastic body

where:

$\partial\Omega = \partial\Omega_t \cup \partial\Omega_u$: total boundary of the body Ω and $\partial\Omega_t \cap \partial\Omega_u = \varnothing$

$\partial\Omega_t$, $\partial\Omega_u$: free and constrained boundary of the body Ω

$\lambda(t)\ \mathbf{t}(\mathbf{x})$: surface loads on the free boundary $\partial\Omega_t$

$\lambda(t)\ \mathbf{b}(\mathbf{x})$: body forces in Ω

$\dot{\mathbf{u}}_g(\mathbf{x},t)$: assigned velocity vector and $\dot{\mathbf{u}}(\mathbf{x},0) = \mathbf{0}$ on $\partial\Omega_u$

$\lambda(t)$: time dependent load multiplier function.

The solution of the elastoplastic problem gives the strain rate $\dot{\mathbf{E}}(\mathbf{x},t)$ and velocity fields $\dot{\mathbf{u}}(\mathbf{x},t)$ satisfying the kinematical admissibility conditions and the stress field $\mathbf{T}(\mathbf{x},t)$ equili-

brated with the applied loads $\lambda(t)\ \mathbf{t}(\mathbf{x})$, $\lambda(t)\ \mathbf{b}(\mathbf{x})$ and the inertial forces $-\mu(\mathbf{x})\ddot{\mathbf{u}}^*(\mathbf{x},t)$, being $\mu(\mathbf{x})$ the mass density function. In the following the approximate response field [34] is assumed in the form:

$$\dot{\mathbf{u}}^*(\mathbf{x},t)=\boldsymbol{\Phi}(\mathbf{x})\,L(t) \tag{1}$$

with:

$$\dot{\mathbf{u}}^*(\mathbf{x},t)=\dot{\mathbf{u}}_g(\mathbf{x},t)\ \text{on}\ \partial\Omega_u\ \ ;\ \dot{\mathbf{u}}^*(\mathbf{x},t)=\mathbf{0}\ \text{in}\ \Omega\ \text{and}\ \partial\Omega_t$$

where the assigned vector $\boldsymbol{\Phi}(\mathbf{x})$ depends on the initial position only and $L(t)$ is an unknown scalar function of the time [35] to be determined.

The difference between the real stress field and the approximate one is in balance with the variation of the associate force fields, reduced to the difference between the inertial forces.

The problem solution does not require that $\mathbf{T}^*(\mathbf{x},t)$ and $\dot{\mathbf{E}}^*(\mathbf{x},t)$ are associated by the plastic law, so that the stress field is dynamically admissible with respect to the D'Alembert principle.

Applying the principle of virtual power

$$\int_\Omega \mu(\ddot{\mathbf{u}}-\ddot{\mathbf{u}}^*)\cdot(\dot{\mathbf{u}}-\dot{\mathbf{u}}^*)\,d\Omega+\int_\Omega(\mathbf{T}-\mathbf{T}^*)\cdot(\dot{\mathbf{E}}-\dot{\mathbf{E}}^*)\,d\Omega=0 \tag{2}$$

and stating

$$\Delta(t)=\frac{1}{2}\int_\Omega \mu(\dot{\mathbf{u}}-\dot{\mathbf{u}}^*)\cdot(\dot{\mathbf{u}}-\dot{\mathbf{u}}^*)\,d\Omega \tag{3}$$

the first derivative of $\Delta(t)$ is calculated:

$$\frac{d\Delta}{dt}=\int_\Omega \mu(\ddot{\mathbf{u}}-\ddot{\mathbf{u}}^*)\cdot(\dot{\mathbf{u}}-\dot{\mathbf{u}}^*)\,d\Omega \tag{4}$$

In view of (4) and (2) it has:

$$\frac{d\Delta}{dt}=-\int_\Omega(\mathbf{T}-\mathbf{T}^*)\cdot(\dot{\mathbf{E}}-\dot{\mathbf{E}}^*)\,d\Omega=0$$

thus:

$$\frac{d\Delta}{dt}=-\int_\Omega\left[(\mathbf{T}-\mathbf{T}^*)\cdot\dot{\mathbf{E}}^*+(\mathbf{T}^*-\mathbf{T})\cdot\dot{\mathbf{E}}^*\right]d\Omega=\int_\Omega\left[(\mathbf{T}^*-\mathbf{T})\cdot\dot{\mathbf{E}}+(\mathbf{T}-\mathbf{T}^*)\cdot\dot{\mathbf{E}}^*\right]d\Omega \tag{5}$$

The stress field $\mathbf{T}$ and the strain rate $\dot{\mathbf{E}}$ are associated through the plastic flow rule, while $\mathbf{T}^*$ satisfies the plasticity condition. The Drucker's stability postulate holds:

$$(\mathbf{T}-\mathbf{T}^*)\cdot\dot{\mathbf{E}}\geq 0\,. \tag{6}$$

In the regions where $\dot{\mathbf{E}}^*(\mathbf{x},t)\neq\mathbf{0}$, the generalized stress field $\mathbf{T}^*_{\dot{\mathbf{E}}^*}$ associated to $\dot{\mathbf{E}}^*$ through the flow rule satisfies the plasticity condition:

$$(\mathbf{T}^*_{\dot{\mathbf{E}}^*}-\mathbf{T})\cdot\dot{\mathbf{E}}^*\geq 0\,. \tag{7}$$

By Drucker's stability postulate the equation (5) may therefore be put in the form:

$$\frac{d\Delta}{dt}=\int_\Omega\left[(\mathbf{T}^*-\mathbf{T})\cdot\dot{\mathbf{E}}+(\mathbf{T}-\mathbf{T}^*)\cdot\dot{\mathbf{E}}^*\right]d\Omega= \tag{8.a}$$

$$= \int_{\Omega} (\mathbf{T}^* - \mathbf{T}) \cdot \dot{\mathbf{E}}\, d\Omega + \int_{\Omega} (\mathbf{T} - \mathbf{T}^*_{\dot{\mathbf{E}}^*}) \cdot \dot{\mathbf{E}}^*\, d\Omega + \int_{\Omega} (\mathbf{T}^*_{\dot{\mathbf{E}}^*} - \mathbf{T}^*) \cdot \dot{\mathbf{E}}^*\, d\Omega \leq \tag{8.b}$$

$$\leq \int_{\Omega} (\mathbf{T}^*_{\dot{\mathbf{E}}^*} - \mathbf{T}^*) \cdot \dot{\mathbf{E}}^*\, d\Omega = \Gamma(t) \;\Rightarrow\; \Gamma(t) \geq 0 \tag{8.c}$$

where the first and the second integral in 8(b) are both less or equal to zero, hence the last term in (8.c) results non-negative, so that:

$$\frac{d\Delta}{dt} \leq \Gamma(t)\,. \tag{9}$$

The integration of the previous relation from 0 to time t gives the approximation measure $\Delta(t)$:

$$\Delta(t) \leq \Delta^+(t) = \int_0^t \Gamma(t)\, dt\,. \tag{10}$$

The maximum value Δ_m of the non decreasing time function $\Delta^+(t)$ is $\Delta^+(T)$, being T the duration of the external forcing function. The function $L(t)$ satisfies the initial conditions:

$$L(0) = 0\,. \tag{11}$$

Due to the condition $\dot{\mathbf{u}}^*(\mathbf{x},0) = 0$. If $\boldsymbol{\Psi}(\mathbf{x})$ is the vector involving the strain generalized components associated to modal vector $\boldsymbol{\Phi}(\mathbf{x})$, the acceleration $\ddot{\mathbf{u}}^*(\mathbf{x},t)$ and the strain rate $\dot{\mathbf{E}}^*$ are given by:

$$\ddot{\mathbf{u}}^*(\mathbf{x},t) = \boldsymbol{\Phi}(\mathbf{x})\, \dot{L}(t) \quad ; \quad \dot{\mathbf{E}}^*(\mathbf{x},t) = \boldsymbol{\Psi}(\mathbf{x})\, L(t) \tag{12}$$

The principle of virtual velocity gives:

$$\int_{S_L} \mathbf{p}(\mathbf{x},t) \cdot \dot{\mathbf{u}}^*\, dS + \int_{\Omega} [\mathbf{F}(\mathbf{x},t) - \mu \ddot{\mathbf{u}}^*] \cdot \dot{\mathbf{u}}^*\, d\Omega = \int_{\Omega} \mathbf{T}^*(\mathbf{x},t) \cdot \dot{\mathbf{E}}^*(\mathbf{x},t)\, d\Omega \tag{13}$$

that can be manipulated with reference to (1) and (12):

$$\int_{S_L} \mathbf{p}^T(\mathbf{x},t)\, \boldsymbol{\Phi}(\mathbf{x}) dS + \int_{\Omega} \mathbf{F}^T(\mathbf{x},t)\, \boldsymbol{\Phi}(\mathbf{x}) d\Omega =$$
$$= \dot{L}(t) \int_{\Omega} \mu(\mathbf{x})\, \boldsymbol{\Phi}^T(\mathbf{x})\, \boldsymbol{\Phi}(\mathbf{x}) d\Omega + \int_{\Omega} \mathbf{T}^*(\mathbf{x},t)\, \boldsymbol{\Psi}(\mathbf{x}) d\Omega$$

so that the function $L(t)$ can be evaluated by integration of the following function:

$$\dot{L}(t) = \frac{\int_{S_L} \mathbf{p}^T(\mathbf{x},t)\, \boldsymbol{\Phi}(\mathbf{x}) dS + \int_{\Omega} \mathbf{F}^T(\mathbf{x},t)\, \boldsymbol{\Phi}(\mathbf{x}) d\Omega - \int_{\Omega} \mathbf{T}^*(\mathbf{x},t)\, \boldsymbol{\Psi}(\mathbf{x}) d\Omega}{\int_{\Omega} \mu(\mathbf{x}) \boldsymbol{\Phi}^T(\mathbf{x})\, \boldsymbol{\Phi}(\mathbf{x}) d\Omega}\,. \tag{14}$$

This method can be applied to pulse loads, with the two conditions that the tractions applied to $\partial\Omega_t$ are null and the initial velocities are prescribed over the whole structure at time $t = 0$; therefore, no external forces do work on the structure.

3 THE WIND TURBINE SDOF MODEL

Dynamic behaviour of wind turbine towers can be easily represented by that of a cantilever beam supported at the base, with all the advantages of a single-degree-of-freedom (SDOF) model. The problem is one-dimensional, so that parameters and relations developed in the

previous section become scalar. The Cartesian reference frame has the origin in the support section and the z axis coincident with the wind tower axis (Figure 2a). The local yield kinematism corresponds to the activation of a shear hinge in which the total shear force $T(z,t)$ attains its bound value. The mechanical characteristics are shown in Figure 3b and 3c:

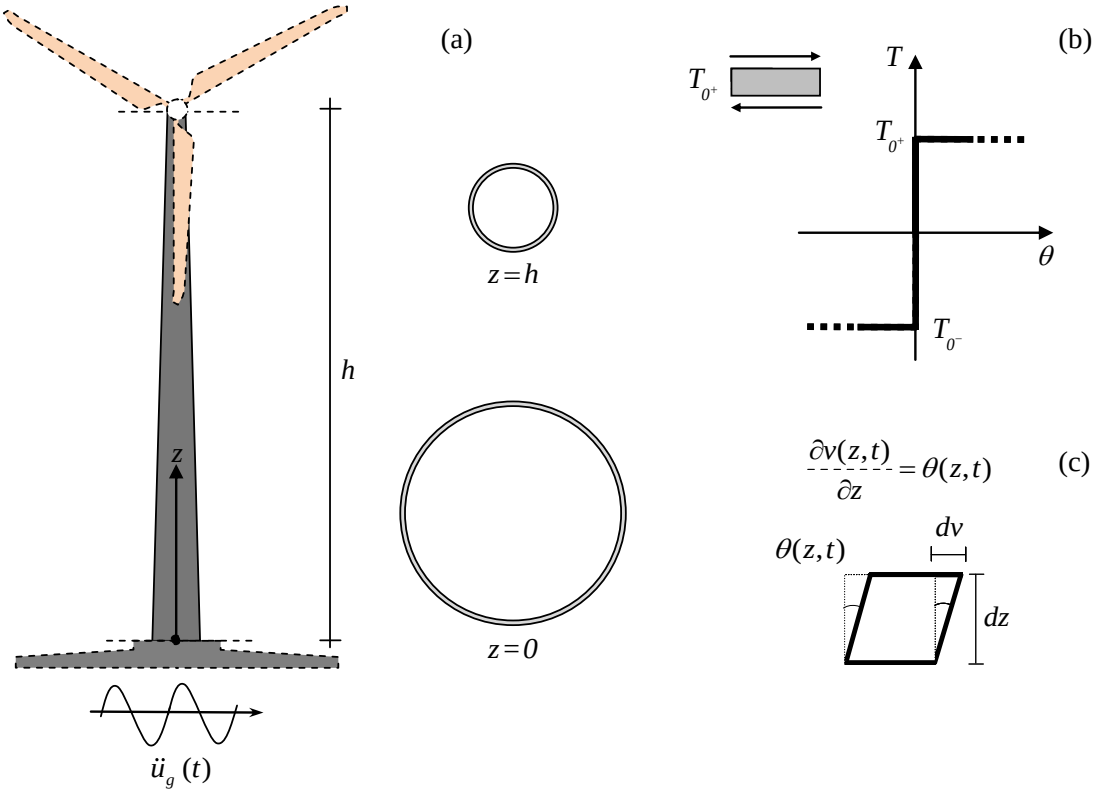

Figure 3: Wind turbine tower geometry (a), rigid-plastic constitutive law (b) and shear strain representation (c)

where:

$\mu(z)$: linear mass density of the tower

$u_g(t)$: horizontal motion of the supported section

$T(z,t)$: shear stress whose bounds are $T_{0^+}(z)$ and $T_{0^-}(z)$

$\theta(z,t)$: shear strain

h: total length of the tower.

The shear plastic constitutive relations are the following:

$$\begin{cases} \left[T(z,t)-T_{0^+}(z)\right]\left[T(z,t)+T_{0^-}(z)\right]\dot{\theta}(z,t)=0 \\ -T_{0^-}(z)\le T(z,t)\le T_{0^+}(z) \end{cases} \tag{15}$$

that is

$$\begin{aligned} -T_{0^-}<T<T_{0^+} \quad & \dot{\theta}=0 \quad \Rightarrow \quad \left[T-T_{0^+}\right]\dot{\theta}=0 \ \text{ and } \ \left[T+T_{0^-}\right]\dot{\theta}=0 \\ T=T_{0^+} \quad & \dot{\theta}\neq 0 \quad \Rightarrow \quad \left[T-T_{0^+}\right]\dot{\theta}=0 \\ T=-T_{0^-} \quad & \dot{\theta}\neq 0 \quad \Rightarrow \quad \left[T+T_{0^-}\right]\dot{\theta}=0. \end{aligned}$$

where the plastic strain rate $\dot{\theta}$ depends on the shear stress only. The dynamic equilibrium equation in the cross section at the z level involves the inertial forces only:

$$\frac{\partial T(z,t)}{\partial z} = \mu(z)\ddot{u}(z,t) = \mu(z)[\ddot{u}_g(t) + \ddot{v}(z,t)]. \tag{16}$$

where:

$$u(z,t) = u_g(t) + v(z,t), \tag{17}$$

is the absolute displacement and:

$$v(z,t) = \int_0^z \theta(x,t)dx = \int_0^z \int_0^t \dot{\theta}(x,\tau)d\tau\, dx \tag{18}$$

is the relative one. A plastic shear hinge occurs when the limit value of shear stress is reached. One or more shear hinges can be activated in the sections z_1, z_2, ..., z_n during the plastic phase, and their abscissa varies according to the time. The kinematic compatibility states that the plastic strain rate is non null in the active hinges only:

$$v(z,t) \qquad \dot{\theta}(z,t) = \frac{\partial \dot{v}(z,t)}{\partial z} = \dot{v}'(z,t). \tag{19}$$

The relative displacement in (18) can be deduced integrating (19) with respect to z and introducing the Heaviside function $H(z)$ ($H(z)=0$ for $z<0$, $H(z)=1$ *for* $z\geq 0$):

$$v(z,t) = \int_0^z v'(x,t)\,dx = \int_0^z \theta(x,t)\,dx = \int_0^h \theta(x,t)H(z-x)\,dx. \tag{20}$$

A double time derivation gives the relative acceleration $\ddot{v}(z,t)$:

$$\ddot{v}(z,t) = \int_0^z \ddot{\theta}(x,t)\,dx = \int_0^h \ddot{\theta}(x,t)H(z-x)\,dx \tag{21}$$

In case of only one shear hinge active the time dependent position is denoted with $z_0(t)$, so the relative displacement velocity and the plastic strain rate have the form:

$$\dot{v}(z,t) = \dot{v}_1(t)H[z - z_0(t)]$$

$$\dot{\theta}(z,t) = \dot{v}'(z,t) = \dot{v}_1(t)\ \delta[z - z_0(t)]$$

being $\delta[z - z_0(t)]$ the Dirac function relative to the plastic hinge position. The shear stress become:

$$T(z,t) = \ddot{u}_g(t)\int_h^z \mu(x)\,dx + \int_h^z \mu(x)\ddot{v}(x,t)dx = \ddot{u}_g(t)\int_h^z \mu(x)\,dx + \ddot{v}_1(t)\int_h^z \mu(x)H[x - z_0(t)]dx$$

The mass functions are:

$$m(z) = \int_h^z \mu(x)\,dx \quad ; \quad m_H[z, z_0(t)] = \int_h^z \mu(x)H[x - z_0(t)]\,dx \tag{22}$$

the time derivative of the second relation (22) gives:

$$\frac{\partial m_H[z,z_0(t)]}{\partial t} = -\mu(z)\,\dot{z}_0(t)H[z-z_0(t)] = -\dot{z}_0(t)\frac{\partial m_H[z,z_0(t)]}{\partial z}.$$

The shear stress and its derivatives in function of the masses are:

$$T(z,t) = \ddot{u}_g(t)\,m(z) + \ddot{v}_1(t)\,m_H[z,z_0(t)]$$

$$\frac{\partial T(z,t)}{\partial z} = \mu(z)\,\ddot{u}_g(t) + \ddot{v}_1(t)\frac{\partial m_H[z,z_0(t)]}{\partial z}$$

$$\frac{\partial T(z,t)}{\partial t} = m(z)\,\dddot{u}_g(t) + \dddot{v}_1(t)\,m_H[z,z_0(t)] - \dot{z}_0(t)\,\ddot{v}_1(t)\frac{\partial m_H[z,z_0(t)]}{\partial z}.$$

The approximation by the Taylor series of the shear stress is:

$$\begin{aligned} T(z_0+dz_0,t+dt) = T(z_0,t) &+ \left\{\mu(z_0)\,\ddot{u}_g(t) + \ddot{v}_1(t)\frac{\partial m_H[z,z_0(t)]}{\partial z}\bigg|_{z=z_0}\right\}dz_o + \\ &+ \left\{m(z_0)\,\dddot{u}_g(t) + \dddot{v}_1(t)\,m_H[z_0,z_0(t)] - \ddot{v}_1(t)\,\dot{z}_0(t)\frac{\partial m_H[z,z_0(t)]}{\partial z}\bigg|_{z=z_0}\right\}dt. \end{aligned} \tag{23}$$

taking in mind that in the plastic hinge the shear is equal to the yield value $T(z_0,t) = T_0(z)$. Indeed, if at the instant $t+dt$ the position of the plastic shear hinge is z_0+dz_0, it must be also $T(z_0+dz_0,t+dt) = T_0(z_0+dz_0)$, and $T(z_0+dz_0,t+dt) = T_0(z_0)+T_0'(z_0)\,dz_0$. The equation (23) in this case is more conveniently written as:

$$\begin{aligned} &\left\{\mu(z_0)\,\ddot{u}_g(t) + \ddot{v}_1(t)\frac{\partial m_H[z,z_0(t)]}{\partial z}\bigg|_{z=z_0}\right\}dz_0 + \\ &+ \left\{m(z_0)\,\dddot{u}_g(t) + \dddot{v}_1(t)\,m_H[z_0,z_0(t)] - \ddot{v}_1(t)\,\dot{z}_0(t)\frac{\partial m_H[z,z_0(t)]}{\partial z}\bigg|_{z=z_0}\right\}dt = T_0'(z_0)\,dz_0 \end{aligned} \tag{24}$$

and being $\dot{z}_0 = \dfrac{dz_0}{dt}$, it is:

$$[\mu(z_0)\,\ddot{u}_g(t) - T_0'(z_0)]\;\dot{z}_0(t) + m(z_0)\,\dddot{u}_g(t) + \dddot{v}_1(t)\,m_H[z_0,z_0(t)] = 0\,.$$

By equation (22) the time evolution of the plastic shear hinge is governed by the relation:

$$\dot{z}_0(t) = -\frac{m(z_0)\,\dddot{u}_g(t) + \dddot{v}_1(t)\,H(0)\,m[z_0(t)]}{\mu(z_0)\,\ddot{u}_g(t) - T_0'(z_0)}. \tag{25}$$

When the plastic hinge moves, residual plastic deformations $\theta_r(z_0,t)$ can be detected in the previous position:

$$\theta_r(z_0,t) = \frac{\dot{v}_1(t)}{\dot{z}_0(t)}$$

and their value do not vary until the plastic hinge forms again at the same position. Hence the acceleration $\ddot{v}(z,t)$ can be determined as functions of the shear:

$$T'(z,t) = T'_{0^+}(z) \Rightarrow \ddot{v}(z,t) = \frac{T'_{0^+}(z)}{\mu(z)} - \ddot{u}_g(t)$$
$$T'(z,t) = T'_{0^-}(z) \Rightarrow \ddot{v}(z,t) = \frac{T'_{0^-}(z)}{\mu(z)} - \ddot{u}_g(t).$$

At the abscissa z the inertial force:

$$q(z) = -\mu(z)[\ddot{u}_g(t) + \int_0^z \ddot{\theta}(x,t)\,dx]$$

allows the total shear written as:

$$T(z,t) = -\int_h^z q(x)\,dx = \ddot{u}_g(t)\,m(z) + \int_h^z \mu(x)\int_0^x \ddot{\theta}(y,t)\,dy\,dx. \tag{26}$$

The (26) can be put after some algebraic manipulations [7] in the form:

$$\begin{aligned} &[\ddot{u}_g(t) + \int_0^{z_1} \ddot{\theta}(y,t)\,dy - \frac{T_{0^+}(z_1)}{m(z_1)}][\ddot{u}_g(t) + \int_0^{z_1} \ddot{\theta}(y,t)\,dy - \frac{T_{0^-}(z_1)}{m(z_1)}] = 0 \\ &\frac{T_{0^-}(z)}{m(z)} < \ddot{u}_g(t) + \int_0^{z_1} \ddot{\theta}(y,t)\,dy < \frac{T_{0^+}(z)}{m(z)} \quad , \quad \forall z > z_1 \end{aligned} \tag{27}$$

According the (27) the plastic deformations stop at the abscissa z_p and cannot propagate upward. The abscissa z_p can be obtained solving a minimum problem independent on time *t* and on ground acceleration $\ddot{u}_g(t)$:

$$\left.\begin{aligned} z_{p1} \rightarrow \frac{T_{0^+}(z_{p1})}{m(z_{p1})} &= \min_{z\in(0,h)}\left[\frac{T_{0^+}(z)}{m(z)}\right] \\ z_{p2} \rightarrow \frac{T_{0^-}(z_{p2})}{m(z_{p2})} &= \min_{z\in(0,h)}\left[\frac{T_{0^-}(z)}{m(z)}\right] \end{aligned}\right\} \quad \Rightarrow \quad z_p = max(z_{p1}, z_{p2}) \tag{28}$$

when equation (28) is satisfied for $z_p = 0$ the beam response involves only one degree of freedom. A wind turbine tower can be represented by a vertical cantilever beam subjected to harmonic base motion and symmetric yield response of the variable hollow circular cross section in the motion plane [7].

The plastic yield shear is given by:

$$T_0(z) = \tau_0 \frac{\pi\,\delta(z)\,R(z)}{4}\left(4 + \frac{\delta^2(z)}{R^2(z)}\right)$$

where $R(z)$ is the inner radius of the cross section, $\delta(z)$ is its thickness and τ_0 is the material shear yield stress. Considering that the thickness is negligible with regard to the radius, it is possible to express $T_0(z)$ as a quadratic function of *z*, in the hypotheses of linear variation of both $R(z)$ and $\delta(z)$.

The case study is the wind turbine whose geometrical properties are reported in (29):

$$\begin{cases} h = 76.15\,m & (\textit{total height of the tower}) \\ \mu(z) = a\,z^2 + b\,z + c & (\textit{mass linear density}) \\ \textit{with} \quad a = 6.9\times10^{-2}\,kg\,m^{-3} & e = -30\ kg\,m^{-2},\ \ c = 4.904\times10^{3}\,kg\,m^{-1} \\ \ddot{u}_g(t) = a_0 \sin\omega t & (\textit{base motion}) \\ D = 6\ sec & (\textit{duration of the time history}) \\ T_0(z) = d\,z^2 + e\,z + f & (\textit{yield shear}) \\ \text{with} \quad d = 1.944\times10^{3}\ Nm^{-2} & e = -518.61\,Nm^{-1},\ \ f = 3.18\times10^{7}\ N \end{cases} \tag{29}$$

The plastic boundary $z_0(t)$ evolves depending on the harmonic forcing time history. The numerical analyses identify two plastic hinges: the first one near the support (0.5 m) and the second one at 13 m level.

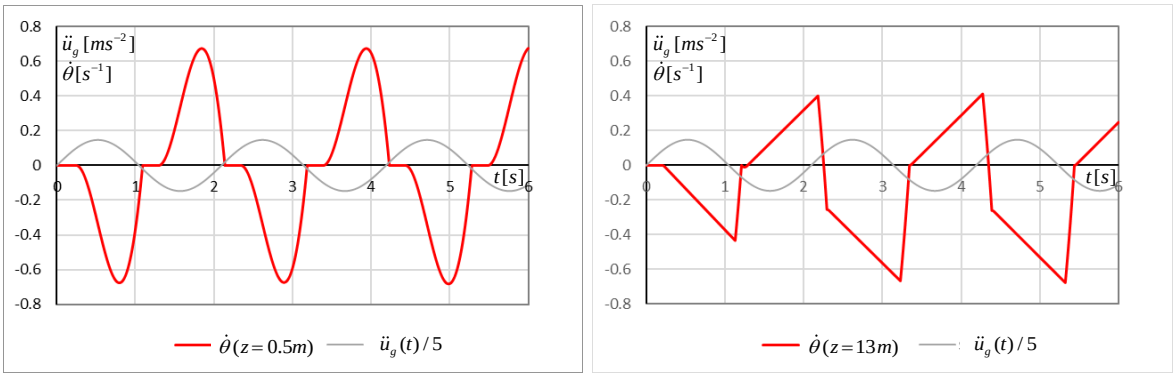

Figure 4: Time histories of the plastic shear strain rate at the base (left) and at the 13 m hinges level (right)

The relative displacements in this last hinge are significantly larger than those evaluated near the support. The time histories of the plastic shear strain rate at the base and at the 13 m level are reported in Figure 4, together with the base acceleration for amplitude $a_0 = 0.3g$ and $f = \dfrac{\omega}{2\pi} = 0.4775\,Hz$ with $\omega = 3\,s^{-1}$. For graphical clarity the scale of the ground acceleration has been reduced. The same parameters have been used for digrams of Figure 5.

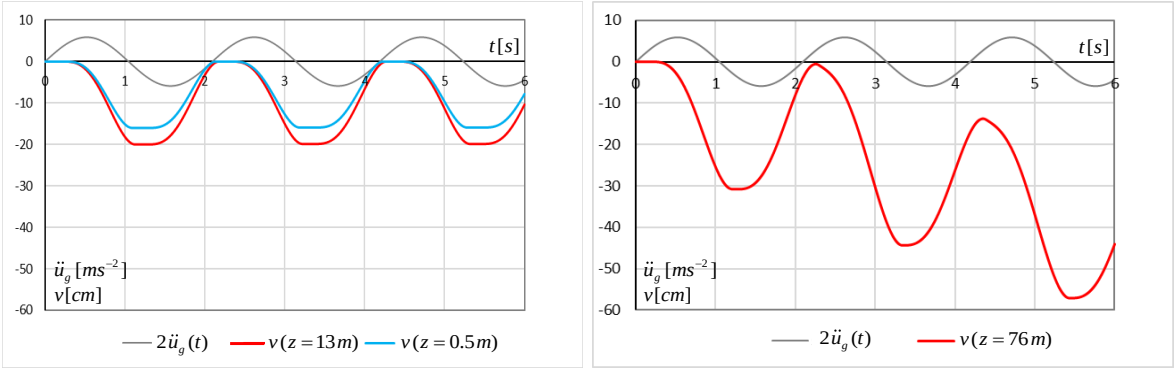

Figure 5 Time histories of the displacement at the plastic hinge levels (left) and at the top of the tower (right)

In Figure 5 the variation of the displacement at the plastic hinge level and at the top of the tower can be detected. As it can be noted the displacements in the range below the 13 m plastic hinge are periodic, while those of the upper part are increasing with the number of cycles. The displacement of the top section of the tower is reported only as an example. Those relative to the other cross sections between the 13 m level and the top one are coincident, due to the simplified constitutive rigid-plastic model, so that the relative displacements curves are coincident with that represented in Figure 5, right, and relative to the top of the tower. The ordinates of the graph relative to the ground acceleration have been doubled to improve reading. In Figure 6 the maximum and minimum displacements versus the amplitude a_0 / g of the base acceleration corresponding to different excitation frequencies are represented.

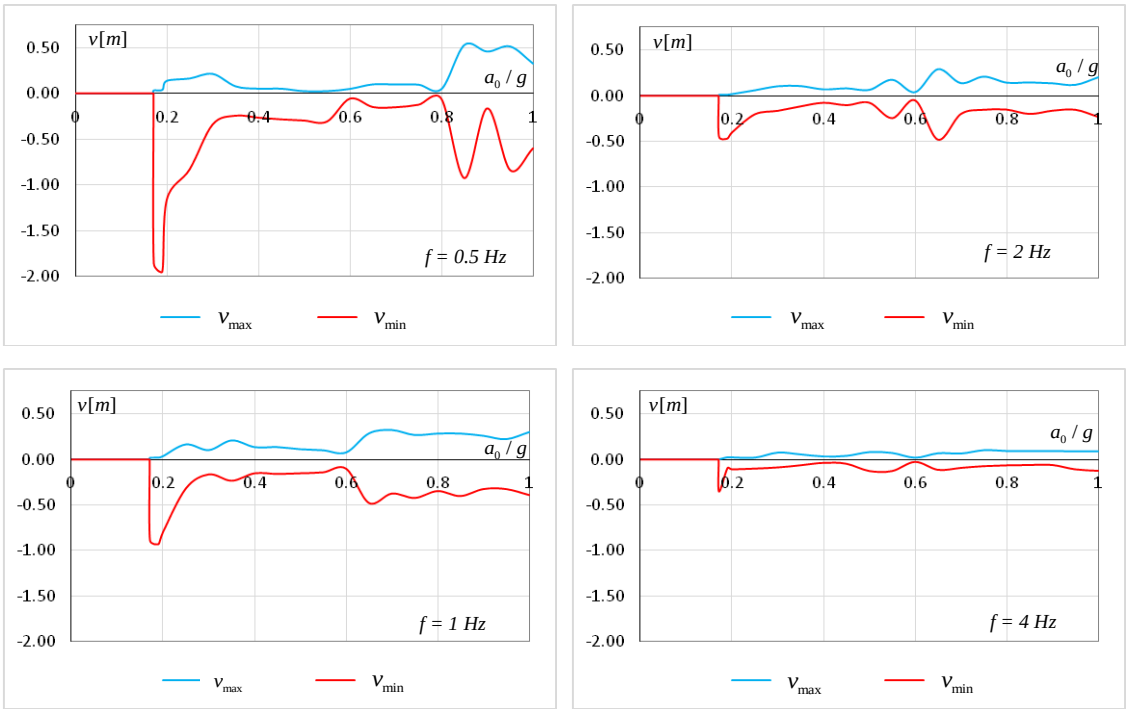

Figure 6: Variation of the maximum and minimum displacement versus the base motion acceleration amplitude corresponding to different frequencies

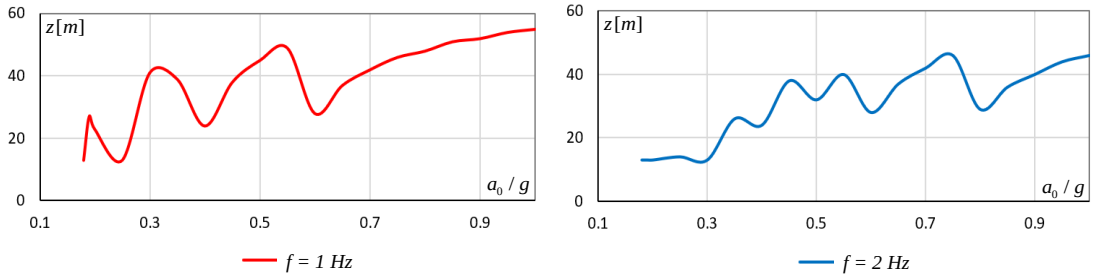

Figure 7: Variation of the plastic hinges position versus amplitude for two different frequencies

The values of both maximum and minimum displacements decrease with increasing frequencies and show in every examined case a peak value at about $a_0 / g = 0.2$. The position of

plastic shear hinges are reported in Figure 7 for two different frequencies. It can be noted that the position of the plastic hinge oscillates in a range variable between 13 m and 55 m..

4 CONCLUSIONS

The dynamic response of a wind turbine tower subjected to inertia forces due to harmonic base motion have been presented in this paper. Failure is considered due to the formation of shear hinges and a step by step integration method is adopted to calculate the dynamic response of the structure in the whole time domain. The procedure allow the representation of the hinge patterns and an estimation of the maximum and minimum displacement under different base motions. The numerical results show that there is a range of frequencies and accelerations that induce large displacements in the tower.

The proposed procedure provides an efficient representation of the tower post-elastic behaviour and a good estimation of the fundamental response modes with the benefit of low computational efforts and limited number of mechanical parameters. This procedure can be extended to steel building structures, since it can provide the localization of damage due to the extension of the plastic front that allows the designer to recognize the segment of structure needing special attention.

5 ACKNOWLEDGEMENTS

The contribute of Ministry of Education, University and Research and particularly the Basic Research Activities Fund (FFABR) is gratefully acknowledged.

REFERENCES

[1] Gesualdo A., Iannuzzo A.**,** Penta F., Monaco M., Nonlinear dynamics of a wind turbine tower, *Front. Mech. Eng.,* doi: 10.1007/s11465-019-0524-3, 2019.

[2] Martin J.B., The determination of mode shapes for dynamically loaded rigid-plastic structures. *Meccanica*, 16(1), 42-45, 1981.

[3] Penta, F., Monaco, M., Pucillo, G.P., Gesualdo, A., Periodic beam-like structures homogenization by transfer matrix eigen-analysis: a direct approach, *Mech. Res. Comm.*, 85, 81-88, 2017.

[4] Gesualdo A., Iannuzzo A., Minutolo V., Monaco M., Rocking of freestanding objects: theoretical and experimental comparisons, *J. Theor. App. Mech-Pol.,* 56(4), 2018.

[5] Augusti G., Rigid-plastic structures subject to dynamic loads. *Meccanica*, 5(2), 74-84, 1970.

[6] Málaga- Chuquitaype C., Elghazouli A. Y., Bento R., Rigid- plastic models for the seismic design and assessment of steel framed structures. *Earthquake Engng. Struct. Dyn.*, 38(14), 1609-1630, 2009.

[7] Rutenberg A., The seismic shear of ductile cantilever wall systems in multistorey structures. *Earthquake Engng. Struct. Dyn.*, 33(7), 881–896, 2004.

[8] Calderoni B., Formisano A., De Martino A., Flexural cyclic behaviour and low-cycle fatigue of cold-formed steel members. *Proc. Final Conf. COST ACTION C12, Innsbruck, Austria*, 301-309, 2005.

[9] Calderoni B., Giubileo C., De Martino A., Assessment of hysteretic cyclic behaviour of plastic hinge in cold-formed steel beams. *Proc. 5th Int. Conf. on behaviour of steel structures in seismic areas, STESSA 2006*, 185-190, 2006.

[10] Krishnan S., Muto M., Mechanism of Collapse of Tall Steel Moment-Frame Buildings under Earthquake Excitation. *J. Struct. Eng.*, 10.1061/(ASCE)ST.1943-541X.0000573, 2012.

[11] Schubak R.B., Anderson D.L., Olson M.D., Simplified dynamic analysis of rigid-plastic beams. *Int. J. Impact Eng.*, 8(1), 27-42, 1989.

[12] Mavroeidis G.P., Papageorgiou A.S., A mathematical representation of near-fault ground motions. *B. Seismol. Soc. Am.*, 93(3), 1099-1131, 2003.

[13] Vassiliou M.S., Makris N., Estimating Time Scales and Length Scales in Pulselike Earthquake Acceleration Records with Wavelet Analysis. *B. Seismol. Soc. Am.*, 101(2), 596-618, 2011.

[14] Li Q.M., Meng H., Pulse loading shape e effects on pressure–impulse diagram of an elastic–plastic, single-degree-of-freedom structural model. *Int. J. Mech. Sci.* 44(9), 1985-1998, 2002.

[15] Gesualdo, A., Guadagnuolo, M., Penta, F., Dynamic shear behaviour of truss towers for wind turbines, *Journal of Physics: Conference Series*, 1141(1). IOP Publishing, 2018.

[16] Cennamo C., Gesualdo A., Monaco M., Shear plastic constitutive behaviour for near-fault ground motion, *J. Eng. Mech.-ASCE*, 143(9), 04017086, 2017.

[17] Symonds P.S., Fleming W.T.Jr., Parkes revisited: on rigid-plastic and elastic-plastic dynamic structural analysis. *Int. J. Impact Eng.*, 2(1), 1-36, 1984.

[18] https://www.dw.com/image/37017119_303.jpg (© by picture-alliance/dpa/P. Endig)